Imaging and Dosimetric Study on Direct Flat-Panel Detector-Based Digital Mammography System

Reena Sharma[1,2], S. D. Sharma[1,2], P. S. Sarkar[2,3], D. Datta[1,2]

[1]Radiological Physics and Advisory Division, Bhabha Atomic Research Centre, [2]Homi Bhabha National Institute, [3]Technical Physics Division, Bhabha Atomic Research Centre (BARC), Mumbai, Maharashtra, India

Abstract

Introduction: Image quality of digital mammography system is generally defined by three primary physical parameters, namely, contrast, resolution, and noise. Quantification of these metrics can be done by measuring objective image quality parameters defined as contrast-to-noise ratio (CNR), modulation transfer function (MTF), and noise power spectra (NPS). **Materials and Methods:** In the present study, various imaging metrics such as CNR, contrast detail resolution, MTF, and NPS were evaluated for a direct flat-panel detector-based digital mammography system following the European Guidelines. Furthermore, system performance relating to both image quality and doses were evaluated using figure of merit (FOM) in terms of CNR^2/mean glandular dose (MGD) under automatic exposure control (AEC) and clinically used OPDOSE operating mode. **Results and Conclusion:** Under AEC mode, FOM values for the 4.5 cm thick BARC polymethyl methacrylate (PMMA) phantom were found to be 15.02, 15.88, and 19.82 at Mo/Mo, Mo/Rh, and W/Rh target/filter (T/F), respectively. Under OPDOSE mode, FOM values were found to 65.32, 11.80, and 1.14 for the BARC PMMA phantom thickness of 2, 4.5, and 8 cm, respectively. Under OPDOSE mode, the calculated MGD values for three Computerized Imaging Reference Systems slab phantoms having total thickness of 7 cm were observed to be 3.03, 2.32, and 1.75 mGy with glandular/adipose tissue compositions of 70/30, 50/50, and 30/70, respectively, whereas for the 2–8-cm thick BARC PMMA phantom, the calculated MGDs were found to be in the range of 0.57–3.32 mGy. All the calculated MGDs values were found to be lower than the acceptable level of dose limits provided in European Guidelines.

Keywords: Contrast-to-noise ratio, contrast-detail mammography, digital mammography, mean glandular dose, modulation transfer function, noise power spectra, phantoms, X-ray

Received on: 08-06-2018 **Review completed on:** 08-10-2018 **Accepted on:** 09-10-2018

Introduction

In India, use of digital mammography has increased rapidly due to its several advantages over screen-film-based mammography. Digital mammography technology offers simplified archival, retrieval and transmission of images, reduction in mean glandular dose (MGD), higher patient workflow, and improved diagnostic accuracy.[1,2] Digital mammography utilizes digital detectors having the wider dynamic range and is categorized on the basis of direct and indirect flat-panel detector technology. Digital detectors (even with a lower spatial resolution than film) also appear to improve lesion conspicuity through their improved efficiency of absorption of X-ray photons, a linear response over a wide range of radiation intensities and low system noise.[2] In addition, postprocessing software can be utilized to assist the radiologist in evaluating the images for suspicious findings by altering contrast and brightness automatically or manually. Also in digital mammography system, the images can be displayed in hard and soft copy formats. Other advantage of using digital mammography is that computer-aided detection software can be utilized to highlight the abnormal areas of density, mass, or calcification on the mammogram image.

Image quality characterization of any X-ray-based imaging system is evaluated by measuring three primary physical parameters: contrast, resolution, and noise.[3] Practically, quantification of these metrics can be done by evaluating

Access this article online

Quick Response Code:

Website: www.jmp.org.in

DOI: 10.4103/jmp.JMP_64_18

Address for correspondence: Mrs. Reena Sharma, Radiological Physics and Advisory Division, Bhabha Atomic Research Centre, CT and CRS, Anushakti Nagar, Mumbai - 400 094, Maharashtra, India. E-mail: rmks_sharma@yahoo.com

This is an open access journal, and articles are distributed under the terms of the Creative Commons Attribution-NonCommercial-ShareAlike 4.0 License, which allows others to remix, tweak, and build upon the work non-commercially, as long as appropriate credit is given and the new creations are licensed under the identical terms.

For reprints contact: reprints@medknow.com

How to cite this article: Sharma R, Sharma SD, Sarkar PS, Datta D. Imaging and dosimetric study on direct flat-panel detector-based digital mammography system. J Med Phys 2018;43:255-63.

objective image quality parameters defined as contrast-to-noise ratio (CNR), modulation transfer function (MTF), and noise power spectra (NPS).[3] CNR defines the image contrast of a digital imaging system. In addition, CNR measurement is very useful for assessing the performance of automatic exposure control (AEC) system that can be related to the effect on threshold object thickness of a given system.[4] In the present study, we have evaluated the image quality of direct flat-panel-based mammography systems by measuring CNR values under clinically used operating conditions following the European protocol.[5,6] Present days, a new concept called as figure of merit (FOM) is used as a tool in digital mammography to assess the performance in terms of image quality and patient doses.[7,8] FOM of digital mammography system was evaluated in terms of CNR^2/MGD under AEC and clinically used OPDOSE mode using indigenously made polymethyl methacrylate (PMMA) phantom having different thicknesses.[7-9] OPDOSE mode selects the best target/filter combination depending on breast thickness, density, whereas AEC mode selects optimized exposure parameters for each individual breast size and composition and determines the dose based on the contrast needed for the image. European guidelines for quality control (QC) in full-field digital mammography recommends to measure the threshold contrast (i.e., the lowest contrast value for which the objects are visible) visibility under clinical conditions which is used to express the image quality.[10] Furthermore, several studies have also reported that measurement of contrast detail (CD) resolution of the digital mammography system is also an essential part as it helps to visualize the objects with very small contrast and diameter from the background.[11-20] CD resolution studies on the digital mammography system simulating the clinical operating conditions were carried out using the Artinis make contrast-detail mammography (CDMAM 3.4) phantom.

MTF measurement describes the sharpness of digital imaging detector at different spatial frequencies and gives the quantitative analysis of spatial resolution.[21] Various methods have been employed for deriving MTF quantity which is based on slit, edge, and bar pattern.[21-23] In this paper, we report an edge method which was used for deriving MTF of a direct digital mammography imaging system. NPS measurement of digital mammography system describes the noise amplitude and texture observed in images obtained with a uniform field of radiation.[24-30] Under NPS measurement, variance of image intensity divided among its frequency components is calculated from region of interest (ROI) taken from a region of a uniformly exposed image. In the present study, we have evaluated NPS from the uniformly exposed digital mammography images following the European Guidelines.[23]

Estimation and optimization of MGD is an important component of the QC program in mammography due to associated risk of radiation-induced carcinogenesis.[31] Furthermore, in the case of digital mammography, single-dose measurement at one thickness is not sufficient and it requires different PMMA thicknesses and breast-simulating phantoms to measure the radiation doses.[9,32] Hence, MGDs for the digital mammography system was measured using different breast tissue-simulating phantoms.

Materials and Methods

Digital mammography X-ray machine

Mammomat Inspiration digital mammography machine (Siemens Medical Systems, Germany) was employed for all the measurements. The Mammomat Inspiration is DR-based mammography machine which contains Molybdenum (Mo) and Tungsten (W) targets. This machine also contains different filters, namely, 30 µm Mo for Mo target, 25 µm rhodium (Rh) for Mo target, and 50 µm Rh for W target. The operating kilovoltage of the machine is in the range of 23–35 kV at an increment of 1 kV and the focus-to-imager distances are 65.0 cm 65.55 cm for Mo and W targets, respectively. Exposure modes available with the machine are OPDOSE, AEC, and manual. The image receiver of the machine contains solid-state amorphous selenium (a-Se) detector with pixel size of 85 µm. The detector size is 24 cm × 30 cm, but the irradiation field is automatically collimated to 18 cm × 24 cm when the smaller compression paddle is fitted.

Mammography phantoms

Computerized Imaging Reference Systems (CIRS) mammography research set (012A), CIRS mammography accreditation phantom (015A) supplied by CIRS, Norfolk, Virginia, USA, and in-house developed PMMA phantom (Referred as Bhabha Atomic Research Centre [BARC] PMMA phantom) were used to carry out the dosimetry measurements with digital mammography systems.[9,33] Physical and dimensional details of these phantoms are given in Table 1. The CIRS mammography research set contains three different breast tissue equivalent phantoms having semispherical shapes and total thicknesses of 4, 5, and 6 cm. The relative contents of the glandular and adipose tissues of these phantoms are 50/50%, 30/70%, and 20/80%, respectively. CIRS research set also includes 10 cm × 12.5 cm photo timer compensation plates with varying thicknesses (0.5 cm to 7 cm) and varying relative contents of glandular and adipose tissues (30/70%, 50/50%, and 70/30%). The material used in the CIRS phantoms is epoxy resin which mimics the photon attenuation coefficients of a range of breast tissues. The BARC mammography phantom is made up of PMMA and was used for measuring CNR of the digital mammography system at various thicknesses. The BARC mammography phantom is equivalent to commercially available mammography phantoms and considered to be suitable for measuring radiation doses in different breast equivalent thicknesses.[9]

For CD resolution study of digital mammography machine, CDMAM phantom (CDMAM 3.4) along with automated CDMAM Analyzer software V 1.2 (Artinis Medical Systems, The Netherlands) was used.[10] The phantom is delivered with set of five PMMA blocks of different thicknesses ranging from 5 mm to 10 mm and physical dimensions of 180 mm × 240 mm. The CDMAM phantom

Table 1: Physical and dimensional details of different mammography imaging and dosimetry phantoms

Phantom type (glandular/adipose)	Descriptions	Quantity (nos)	Material
CIRS mammography research set (012A)			
CIRS 30/70 slabs (cm^3)	Slab dimensions: 10×12.5×0.5	2	Epoxy resin
	Slab dimensions: 10×12.5×1.0	2	
	Slab dimensions: 10×12.5×2.0	2	
CIRS 50/50 slabs (cm^3)	Slab dimensions: 10×12.5×0.5	2	
	Slab dimensions: 10×12.5×1.0	2	
	Slab dimensions: 10×12.5×2.0	2	
CIRS 70/30 slabs (cm^3)	Slab dimensions: 10×12.5×0.5	2	
	Slab dimensions: 10×12.5×1.0	2	
	Slab dimensions: 10×12.5×2.0	2	
CIRS 10 B	Tissue equivalent mammography phantom, 4 cm thickness having 50% glandular tissue and 50% adipose tissue	1	
CIRS 10 A	Tissue equivalent mammography phantom, 5 cm thickness having 30% glandular tissue and 70% adipose tissue	1	
CIRS 10 C	Tissue equivalent mammography phantom, 6 cm thickness having 20% glandular tissue and 80% adipose tissue	1	
CIRS mammography accreditation phantom (015A) (cm^3)	Dimensions: 10.8×10.2×4.4	1	PMMA
BARC-PMMA phantom	Semispherical phantom with the length and radius of the central slab of 21 and 10 cm respectively	1	PMMA

CIRS: Computerized Imaging Reference Systems, BARC: Bhabha Atomic Research Centre, PMMA: Polymethylmethacrylate

consists of a 16 cm × 24 cm × 0.3 mm aluminum (Al) plate with 205 square cells (arranged in 16 rows × 16 columns) with gold disks of various thicknesses (0.03 µm to 2.00 µm) and diameters (0.06 mm to 2.00 mm). These disks are aligned on a two-dimensional grid where two disks can be found in each cell, one in the center and another in one of the four cell corners. Columns have equal gold disc thickness whereas rows have equal gold disc diameters. The CDMAM 3.4 phantom was positioned on the bucky of the mammography machine. The structures with the smallest diameter were located closest to the chest wall side of the bucky. PMMA blocks supplied along with CDMAM phantom were used to increase the total thickness of the phantom. CDMAM Analyzer software was used for computing the CD curve, the inverse image quality figure (IQF_{inv}) and % detected gold disks, which offers the various functionality test on the exposed CDMAM 3.4 phantom images which should be DICOM (digital imaging and communications in medicine) tagged.[10] CDMAM analyzer software offers the possibility to analyze more than one CDMAM image into one result thus reducing the influence of image noise.[10] For image quality evaluation, smallest thickness of the disks just visible for each diameter called the threshold contrast was measured using automatic software analyzer and same was plotted in CD curve for the various clinically used operating conditions. The IQF_{inv} numbers were obtained from the analyzed CDMAM phantom images which determines the contrast (thickness) threshold in the image of the object as a function of the detail (diameter) and is calculated using given equation 1.

$$IQF_{inv} = \frac{100}{\sum_{i=1}^{16} C_{i,th} \times D_i} \quad (1)$$

Figure 1: Experimental set up for measurement of breast entrance exposure in mammography phantom

where $C_{i,th}$ denotes the threshold thickness in diameter-column i and Di denotes the threshold diameter in contrast column i. The contrast is given in "µm" whereas the diameter is taken in "mm." Furthermore, % detected disks were obtained from the analyzed CDMAM phantom image which is also used as the image quality indicator. Higher the IQF_{inv}, better the low contrast visibility.

Half value layer (HVL), radiation output, breast entrance exposure, and mean glandular dose measurements

Beam quality (HVL) and radiation output (mGy) measurements at different kVp stations and target/filter combinations were carried out using Raysafe X2 base unit along with Raysafe X2 MAM sensor (Fluke Biomedical, USA) having measurable dose range of 1 μGy to 99.99 Gy with uncertainty of 5%. All these measurements were performed using manual mode digital mammography machine. Raysafe X2 base unit along with Raysafe X2 MAM sensor was also used for measuring breast entrance exposure (BEE) while exposing different mammography phantoms. During BEE measurement, Raysafe X2 MAM sensor was placed at one side of the phantom and compression plate was used in contact of phantom to simulate clinical exposure conditions as shown in Figure 1. The MGD values were calculated from the measured BEEs by applying multiple conversion factors using equation 2.[31,34]

$$MGD = K.\ g.\ c.\ s \quad (2)$$

where *K* represents the BEE (i.e., incident air kerma) at the upper surface of the breast, *g* is the incident air kerma to MGD conversion factor corresponding the glandularity of 50%, *c* is the correction factor for difference in breast composition from 50% glandularity, and *s* is the correction factor for difference in X-ray spectra. Dance *et al*. have given g and c values against HVL of the X-ray beams in the tabulated form.[31,34] Using these standard tables, data points were plotted and same were used to derive the values of *g* and *c* factors corresponding to the HVL values measured for different mammography phantoms for the studied digital mammography system in the present study.

Contrast-to-noise ratio measurement

For CNR measurements, a square plate of aluminum (Al) of dimension 10 mm × 10 mm and thickness 0.2 mm was placed on different thickness of PMMA phantom which ranges from 2 to 8 cm as shown in Figure 2. While carrying out the CNR measurements, BEE was measured using Raysafe X2 MAM sensor positioned by the side of PMMA phantom of different thicknesses and compression paddle in contact of phantom to derive the actual MGD. The images of the different PMMA phantom thicknesses obtained during the dose measurement were analyzed to obtain the CNR values using Image J software.[35] A 5 mm × 5 mm square ROI was used to determine the average signal pixel value (PV_{signal} at location 2, Al) and the standard deviation (SD) in the signal within the image of the Al square and the surrounding background (ROI) at location 1 (PMMA) as shown in Figure 3. The CNR was calculated for each image as defined in the European protocol using the following equation 3.

$$CNR = \frac{PV_{Signal} - PV_{Bkg}}{\sqrt{\frac{(SD_{Signal})^2 + (SD_{Bkg})^2}{2}}} \quad (3)$$

where PV_{signal} is the average pixel value of the signal, PV_{bkg} is the average pixel value of background, SD_{signal} is the SD in the signal area 2, and SD_{bkg} is the SDs in the background area 1.

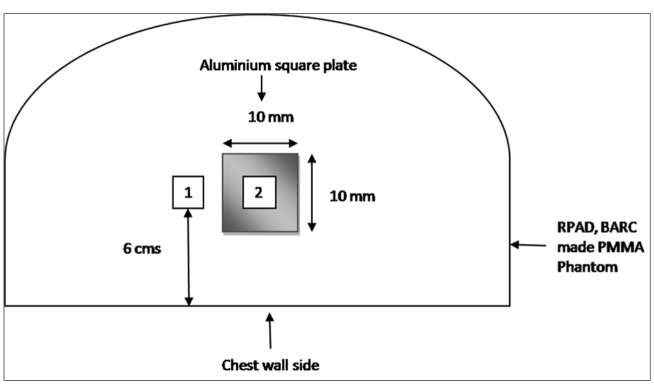

Figure 2: Set up for contrast-to-noise ratio measurement with different BARC polymethyl methacrylate phantom thicknesses

Figure of merit measurements

FOM for the digital mammography system was evaluated using the measured CNR values and corresponding MGDs in BARC mammography PMMA phantom. Equation 4 was used for all the FOM calculation.

$$FOM = \frac{CNR^2}{MGD} \quad (4)$$

Furthermore, percentage change (%) was calculated in terms of increased or decreased value for the three measured parameters called CNR, MGD, and FOM using the formula given by equation 5.

$$\text{Percentage change (\%)} = \frac{[Reference_{value} - Observed_{value}]}{Reference_{value}} \times 100 \quad (5)$$

Modulation transfer function and noise power spectra measurements

MTF of the digital mammography system was measured using a slanted radiopaque edge placed at the detector input plane with grid in position.[21-23] Image of the exposed radiopaque plate is shown in Figure 3. Radiopaque plate was made up of tantalum having sharp and straight edge with dimensions 10 cm × 10 cm and thickness of 100 μm. The edge spread function (ESF) was obtained using Image J software from the image of tantalum

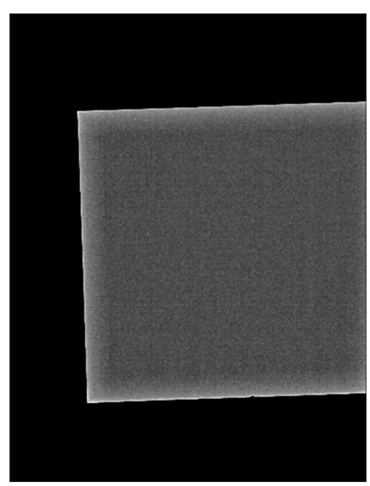

Figure 3: Image of exposed radioopaque tantalum plate used for modulation transfer function measurement

plate. Derivative of the ESF was calculated to generate line spread function (LSF) as given by the following equation.

$$\mathrm{LSF}\ (X) = \frac{d}{dx}\mathrm{ESF}(x) \quad (6)$$

The presampled MTF was obtained from the LSF using fast Fourier transform (FFT) and by calculating the magnitude as given by the following equation.

$$\mathrm{MTF} = |\,\mathrm{FFT}[\mathrm{LSF}(x)]\,| \quad (7)$$

NPS of the digital mammography system was calculated from a series of flat-field images acquired at radiation dose of ~100 μ Gy using the following equation:[23-30]

$$NPS(u,v) = \frac{\Delta x\ \Delta y}{M.256.256}\sum_{m=1}^{M}\Big|\sum_{i=1}^{256}\sum_{j=1}^{256}\big(I(x_i,y_j) - S(x,y)\big) e^{-2\pi i(u_n x_i + v_k y_j)}\Big|^2 \quad (8)$$

where an ROI dimension of 256 × 256 pixels has been used, M is the number of ROIs, Δx is the pixel spacing in the x-direction, Δy is the pixel spacing in the y-direction, I (x, y) are the pixel value data, S (x, y) is a two-dimensional polynomial function used to the entire extracted region used of NPS analysis.

Results and Discussion

For the studied digital mammography machine, measured HVL values for the different T/F combinations are shown in Figure 4. Before measuring HVL values, accuracy of all the kVp stations and different T/F combinations were evaluated which were found to be <±1 kVp. At Mo/Mo setup, the measured HVL range was found to be 0.294 ± 1E-3–0.357 ± 1E-3 for the applied kVp of 23, 25, and 28. At Mo/Rh set up, HVL range was found to be 0.43 ± 0.002–0.473 ± 1E-3 for the applied kVp of 28, 32, and 34. At W/Rh set up, HVL range was found to be 0.56 ± 0.002–0.62 ± 0.002 for the applied kVp of 28, 32, 34, and 35 kVp.

Results of radiation output (mGy) measured at different T/F combinations for the various kVp stations are shown in Figure 5. Radiation output consistency at all kVp stations and different T/F combinations was calculated in terms of coefficient of variation and was found to be < 0.05. For Mo/Mo and T/F, the radiation output was found to be in the range of 1.16–2.15 mGy at 23, 25, and 28 kVp. For Mo/Rh, measured radiation output range was observed to be 1.62–2.84 mGy at 28, 32, and 34 kVp, and for W/Rh, it was found to be 0.639–1.04 mGy at 28, 32, 34, and 35 kVp.

Figure 6 shows the FOM values in terms of CNR^2/MGD for the 4.5 cm thick BARC PMMA phantom exposed under AEC mode at three different T/F combinations. CNR values for the BARC PMMA phantom with total thickness of 4.5 cm were found to be 6.71, 6.17, and 5.27 with MGD values of 3, 2.4, and 1.4 mGy at T/F of Mo/Mo, Mo/Rh, and W/Rh, respectively. These measured CNR values are found to be within the European limiting CNR values.[5,10] Corresponding calculated FOM values were 15.02, 15.88, and 19.82 for these three T/F combinations, respectively. Percentage decreases in MGD values were found to be 20 and 53.33% when T/F was changed from Mo/Mo to Mo/Rh and W/Rh, respectively. Also for comparing two clinical operating mode, that is, AEC (T/F = W/Rh) and OPDOSE (T/F = W/Rh), % change in MGD, CNR, and FOM for the 4.5 cm BARC PMMA phantom were calculated. It is seen from the compared values that percentage increase of 21.43 was found in MGD value for the AEC than OPDOSE mode, whereas in CNR values, % increase of 31.5 was observed for OPDOSE than AEC mode. Furthermore, percentage increase of 40.46 was found in FOM value for the AEC than the OPDOSE mode at same T/F combination. Hence, it is concluded that for the 4.5 cm thick PMMA phantom, AEC mode provides the better image quality and dose performance.

Calculated FOM values for BARC PMMA phantom of different thicknesses and exposed under OPDOSE mode are shown in Figure 7. It is observed that highest CNR

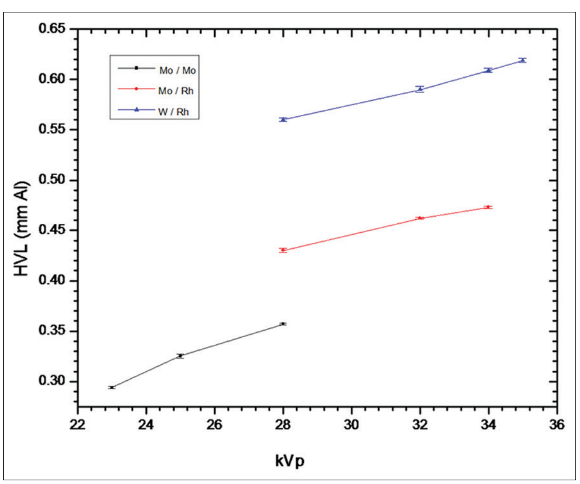

Figure 4: Measured HVL values (mm Al) at different kVp settings for the various target/filter combinations (Mo/Mo, Mo/Rh, W/Rh)

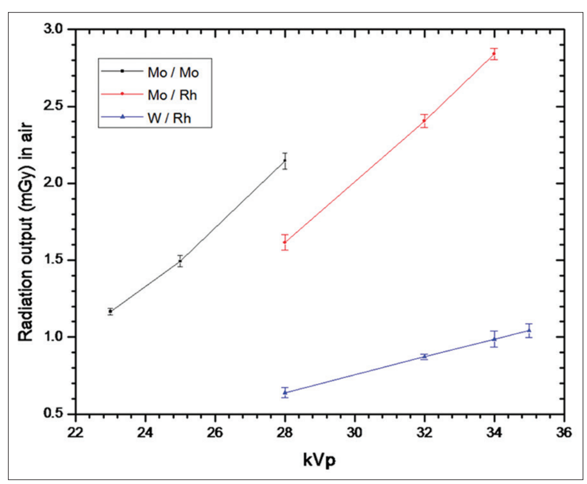

Figure 5: Measured radiation output (mGy) in air at different kVp settings for the various target/filter combinations (Mo/Mo, Mo/Rh, W/Rh)

value with lowest MGD was achieved for 2 cm thick BARC PMMA phantom and lowest CNR with highest MGD value was found to be for 8 cm thick phantom. Correspondingly, highest FOM values were achieved for 2 cm and lowest for 8 cm thick BARC PMMA phantom. The outcome of this analysis suggests that when the breast thicknesses are small, detectability of any mass, or microcalcification will be higher due to higher CNR value observed at lower thickness.

Calculated MGD values for digital mammography system for different breast tissue-simulating phantoms and for different BARC PMMA phantom thickness are given in Tables 2 and 3, respectively. It incorporates the displayed compressed breast thickness (CBT in cm), machine-selected parameters such as T/F combination, applied kVp, mAs, and MGDs. It also include the values of other parameters measured by dosimeter X2 MAM, for example, BEE, HVL, exposure time, and exposure rate. MGD ratio between machine displayed and calculated MGD values using the appropriate conversion factors are also given in Tables 2 and 3. The outcome of the study also show that for the CIRS slabs phantom of different glandular/adipose tissue compositions and physical thickness of 7 cm, the calculated maximum MGD value was found to be of 3.03 for 70/30, 2.32 for 50/50, and 1.75 mGy for the 30/70 glandular/adipose tissue compositions. Furthermore, fitting equation was achieved for the calculated MGD values at different thicknesses of BARC PMMA phantom. The

Table 2: Measured mean glandular dose values under clinically operated OPDOSE mode (target/filter=tungsten/rhodium) for digital mammography system using different breast tissue simulating mammography phantoms

Numbers assigned to phantom types	Phantom type (glandular/adipose)	Quoted physical thickness (cm)	Machine displayed parameters					Dosimeter X2 MAM readings				Calculated MGD (mGy)[31,34]	MGD ratio (machine displayed vs. calculated)
			T/F	CBT (cm)	kVp	mAs	MGD (mGy)	BEE (mGy)	HVL (mm Al)	Exposure time (s)	Exposure rate (mGy/s)		
1	Slabs of CIRS (30/70)	7.0	W/Rh	6.7	30	182.2	1.9	8.53	0.538	2.229	3.825	1.75	1.09
2	Slabs of CIRS (50/50)	7.0	W/Rh	6.7	30	238.6	2.5	11.19	0.54	2.876	3.890	2.32	1.08
3	Slabs of CIRS (70/30)	7.0	W/Rh	6.8	30	311.5	3.3	14.6	0.54	3.360	4.358	3.03	1.09
4	CIRS 10 C	6.0	W/Rh	5.7	29	113.8	1.2	4.67	0.541	1.588	2.941	1.13	1.06
5	CIRS 10 A	5.0	W/Rh	4.7	28	90.4	1.0	3.29	0.537	1.429	2.299	0.96	1.05
6	CIRS 10 B	4.0	W/Rh	3.8	27	75.4	0.9	2.46	0.517	1.426	1.727	0.69	1.30
7	CIRS 015	4.4	W/Rh	4.2	28	81.4	1.2	2.91	0.532	1.417	2.056	1.02	1.18
8	BARC-PMMA	6.0	W/Rh	5.9	29	181	2.1	7.15	0.552	2.241	3.193	1.41	1.49
9	BARC-PMMA	4.5	W/Rh	4.1	28	93.3	1.2	3.35	0.521	1.443	2.322	0.89	1.34

CIRS: Computerized Imaging Reference Systems, BARC: Bhabha Atomic Research Centre, PMMA: Polymethylmethacrylate, T/F: Target/Filter, CBT: Compressed breast thickness, kVp: Kilovoltage peak, mAs: Milliampere second, MGD: Mean glandular dose, BEE: Breast entrance exposure, HVL: Half value layer, mGy: Milli gray, mm Al: Millimeter aluminium, W/Rh: Tungsten/rhodium

Table 3: Measured mean glandular dose values under clinically operated OPDOSE mode (target/filter=tungsten/rhodium) for digital mammography system using Bhabha Atomic Research Centre-polymethylmethacrylate phantom of different thicknesses

BARCPMMA mammography phantom thickness (cms)	Machine displayed parameters			Dosimeter X2 MAM readings				Calculated MGD (mGy)[31,34]	MGD ratio (machine displayed vs. measured)	Acceptable level of dose limits in European guidelines (mGy)[5]
	kVp	mAs	MGD (mGy)	BEE (mGy)	HVL (mm Al)	Exposure time (sec)	Exposure rate (mGy/sec)			
2.0	24	50.7	0.7	1.01	0.490	1.450	0.699	0.57	1.24	<1.0
2.5	26	45.4	0.7	1.21	0.523	1.441	0.842	0.60	1.16	-
3.0	26	58.9	0.8	1.58	0.525	1.462	1.084	0.70	1.15	<1.5
3.5	27	66.9	0.9	2.04	0.535	1.471	1.385	0.81	1.12	-
4.0	27	87.2	1.1	2.71	0.532	1.446	1.875	0.95	1.16	<2.0
4.5	28	98.8	1.3	3.43	0.542	1.502	2.287	1.10	1.18	<2.5
5.0	28	126.8	1.5	4.47	0.543	1.900	2.352	1.31	1.14	<3.0
5.5	29	143.4	1.8	5.59	0.551	2.064	2.711	1.50	1.20	-
6.0	29	181.0	2.1	7.15	0.552	2.241	3.193	1.77	1.19	<4.5
7.0	30	268.9	2.9	11.97	0.557	3.118	3.840	2.58	1.12	<6.5
8.0	31	352.6	3.7	17.59	0.560	3.905	4.505	3.32	1.12	-

BARC: Bhabha Atomic Research Centre, PMMA: Polymethylmethacrylate, kVp: Kilovoltage peak, mAs: Milliampere second, MGD: Mean glandular dose, BEE: Breast entrance exposure, HVL: Half-value layer, mGy: Milligray, mm Al: Millimeter aluminum variation of MGD with BARC PMMA phantom thickness can be represented by the following second-order polynomial fit equation 9.

$$\text{MGD (mGy)} = 0.83 + B_1 \times x + B_2 \times x^2 \quad (9)$$

where "x" represents the thickness of BARC PMAA phantom in centimeter. In equation 9, 0.83 ± 0.09 represents the intercept value with associated standard error of 0.09; B_1 has the value of-0.27 ± 0.04 and B_2 has the value of + 0.072 ± 0.004. Adjusted R-squared value for the fitted data points is found to be 0.99. Establishing this fitted equation will be helpful in deriving the MGDs directly for any value of PMMA thicknesses rather calculating it using measured BEE and conversion factors.

Results of the CD resolution study carried out on digital mammography system are shown in Figures 8 and 9 under different clinical exposure conditions. Figure 8 shows the CD curve for the CDMAM phantom kept on top of the 4.5 cm PMMA sheets and exposed under AEC mode at different T/F combinations. Table 4 gives the detail of image quality parameters analyzed in terms of IQF_{inv} and % detected gold disks from the plotted CD curve along with machine selected and displayed parameters. Figure 9 shows the CD curve plotted for the CDMAM phantom in combination with PMMA sheets of various thicknesses to simulate clinical breast thicknesses in digital mammography. For different exposure conditions, under which CDMAM phantom was exposed, the measured IQF_{inv} numbers and % detected gold disks are presented in Table 5 along with machine selected and displayed parameters.

Figure 10 shows the calculated MTF values at different spatial frequencies from the image of exposed slanted edge device

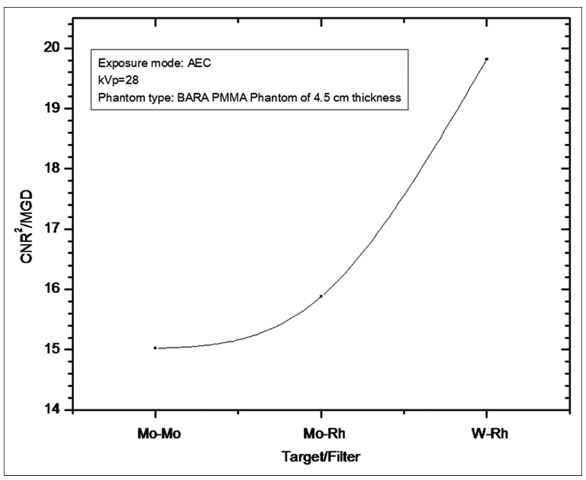

Figure 6: Plot for calculated figure of merit in terms of CNR²/mean glandular dose values for the BARC polymethyl methacrylate phantom with a thickness of 4.5 cm and exposed under automatic exposure control mode

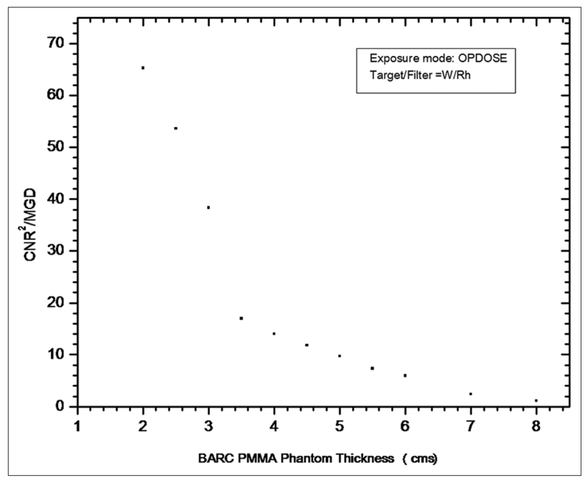

Figure 7: Plot for calculated figure of merit in terms of CNR²/mean glandular dose values for the BARC polymethyl methacrylate phantom having different thicknesses and exposed under clinically used OPDOSE mode

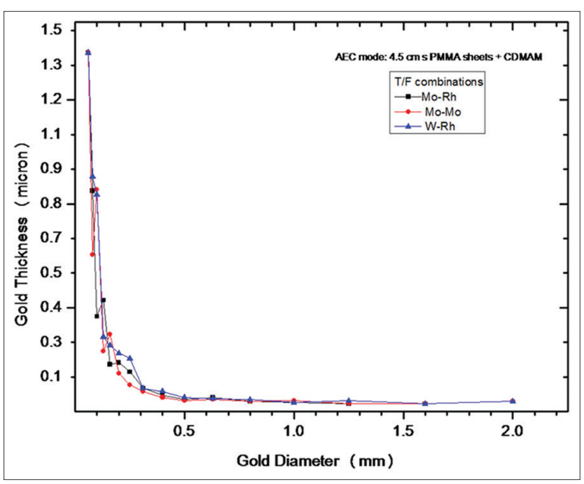

Figure 8: Plot of contrast detail performance for the digital mammography machine using contrast-detail mammography phantom kept on top of 4.5 cm polymethyl methacrylate sheets and exposed under automatic exposure control mode at different target/filter conditions (Mo/Mo, Mo/Rh, W/Rh)

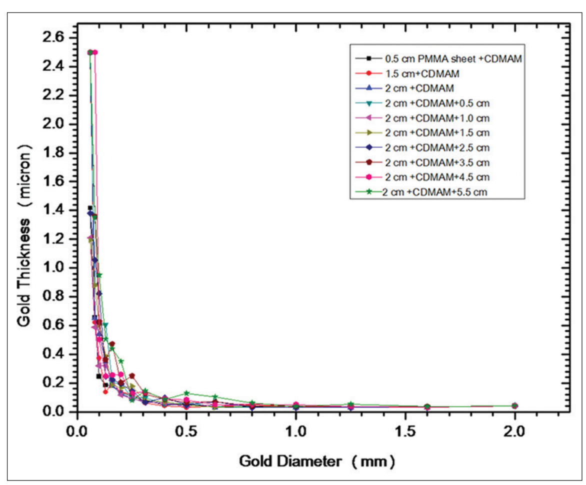

Figure 9: Plot of contrast detail performance for the digital mammography machine using contrast-detail mammography phantom exposed in combination with polymethyl methacrylate sheets of various thicknesses to simulate clinical operating conditions under OPDOSE mode

Table 4: The inverse image quality figure number and % detected gold disks for the contrast-detail mammography phantom which was kept on top of the 4.5 cm thick polymethylmethacrylate sheet and exposed at three different target/filter combinations using automatic exposure control mode

Target filter combination (T/F)	IQF_{inv}	% detected gold disks	Operating parameters (kV/mAs) (average value for eight images)	Machine displayed MGD (mGy)
Mo/Mo	145.7	78.3	28/167.1	3.8
Mo/Rh	144.3	77.4	28/135.2	2.9
W/Rh	127.7	74.5	28/188.9	2.1

T/F: Target/filter, Mo/Mo: Molybdenum/molybdenum, Mo/Rh: Molybdenum/rhodium, W/Rh: Tungsten/rhodium, MGD: Mean glandular dose, mGy: Milligray, IQF_{inv}: Inverse image quality figure, kV: Kilovoltage, mAs: Milliampere second

Table 5: The inverse image quality figure number and percentage detected gold disks for the contrast-detail mammography phantom kept along with polymethylmethacrylate sheets to simulate different clinical breast thicknesses and exposed under clinically used OPDOSE mode

Phantom thickness (cm)	IQF_{inv}	Percentage detected gold disks	Operating parameters (kV/mAs) (average value for eight images)	Machine displayed MGD (mGy)
0.5 PMMA + CDMAM	171.9	81.6	24/41.1	0.6
1.5 PMMA + CDMAM	151.7	79	26/49.6	0.8
2.0 PMMA + CDMAM	144.4	78.7	26/63.2	0.9
2.0 PMMA + CDMAM + 0.5 PMMA	128.1	77.3	27/71.6	1.0
2.0 PMMA + CDMAM + 1.0 PMMA	168.2	79.1	27/97.45	1.25
2.0 PMMA + CDMAM + 1.5 PMMA	147.4	78.5	28/110.3	1.5
2.0 PMMA + CDMAM + 2.5 PMMA	135.6	75.5	29/152.4	2.0
2.0 PMMA + CDMAM + 3.5 PMMA	105.5	71.5	30/206.45	2.4
2.0 PMMA + CDMAM + 4.5 PMMA	102.8	72.0	31/361.3	3.8
2.0 PMMA + CDMAM + 5.5 PMMA	93.6	68.2	32/342.4	3.75

PMMA: Polymethylmethacrylate, CDMAM: Contrast-detail mammography phantom, MGD: Mean glandular dose, mGy: Milligray, IQF_{inv}: Inverse image quality figure

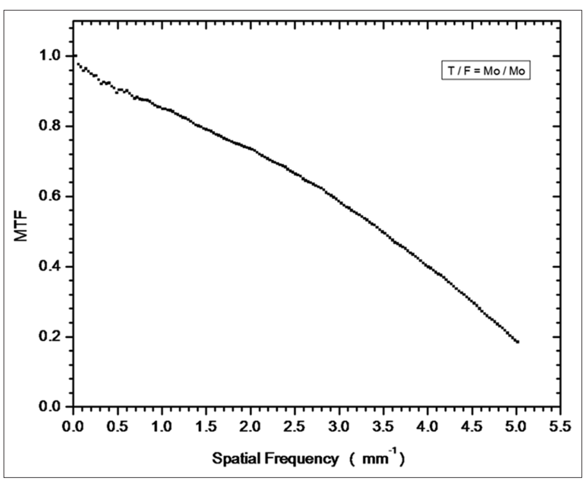

Figure 10: Plot of calculated modulation transfer function values at different spatial frequencies for the digital mammography system

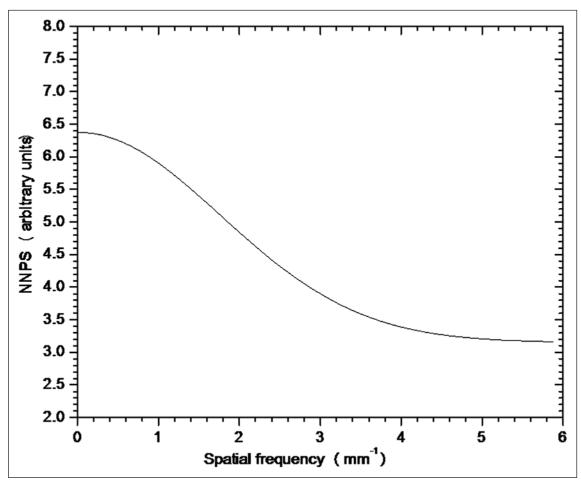

Figure 11: Plot of calculated normalized noise power spectrum for the different spatial frequency at entrance air kerma value of ~100 μ Gy

using Mo/Mo as T/F combination for the digital mammography system. Figure 11 shows the calculated normalized noise power spectrum versus spatial frequency for the digital mammography system at the entrance air kerma of 100 μGy. Both the MTF and the NPS are found to be falling off at higher spatial frequencies. However, at higher spatial frequencies, lower MTF values are observed when compared with reported values for the studied digital mammography machine.

Conclusion

In the present study, various imaging metrics such as CNR, CD resolution, MTF, and NPS were evaluated for a direct flat-panel detector-based digital mammography system following the European Guidelines. As the studied digital mammography system has different exposure mode, a system performance study relating to both image quality and doses was carried out by evaluating FOM in terms of CNR^2/MGD under AEC and clinically used OPDOSE operating mode. Under AEC mode of operation and for a given phantom thickness, the highest CNR and MGD values were observed for Mo/Mo, T/F combination, whereas W/Rh combination has provided the highest FOM value. Whereas, for clinically used OPDOSE mode, highest CNR, lowest MGD, and correspondingly highest FOM values were found for 2 cm thick BARC PMMA phantom. It was also concluded that as the phantom thickness increases, CNR and FOM value decreases. Detailed dosimetric studies were also performed on the digital mammography system by calculating MGDs using several mammography phantoms made up of breast tissue equivalent materials. However, all the calculated MGDs values were found to be lower than the acceptable level of dose limits provided in the European Guidelines.

Financial support and sponsorship

Nil.

Conflicts of interest

There are no conflicts of interest.

References

1. Skaane P. Digital mammography in European population-based screening programs. In: Bick U, Diekmann F, editors. Digital Mammography. Springer, Berlin; 2010. p. 155-73.
2. Tabar L. Imaging of the Breast: Technical Aspects and Clinical Implication. Available from: http://www.intechopen.com/bppks/imaging-of-the-breast-technical-aspects-and clinical-implication. [Last accessed on 2015 Nov 10].
3. Andrew K, Srinivasan V. Detectors for digital mammography. In: Gary JW, Haygood TM, editors. Digital Mammography: A Practical Approach: Cambridge University Press, New York; 2012.
4. Young KC, Engen RV, Bosmans H, Jacobs J, Zanga F. Quality control in digital mammography. In: Bick U, Diekmann F, editors. Digital Mammography. Springer, Berlin; 2010. p. 33-54.
5. Perry N, Broeders M, de Wolf C, Tornberg S, Holland R, von Karsa L. European Guidelines for Quality Assurance in Breast Cancer Screening and Diagnosis. 4th ed. Luxembourg: Renouf Publication Co., Ltd.; 2006. p. 614.
6. Baldelli P, Phelan N, Egan G. A novel method for contrast-to-noise ratio (CNR) evaluation of digital mammography detectors. Eur Radiol 2009;19:2275-85.
7. Borg M, Badr I, Royle GJ. The use of a figure-of-merit (FOM) for optimisation in digital mammography: A literature review. Radiat Prot Dosimetry 2012;151:81-8.
8. Williams MB, Raghunathan P, More MJ, Seibert JA, Kwan A, Lo JY, *et al.* Optimization of exposure parameters in full field digital mammography. Med Phys 2008;35:2414-23.
9. Sharma R, Sharma SD, Mayya YS, Chourasiya G. Mammography dosimetry using an in-house developed polymethyl methacrylate phantom. Radiat Prot Dosimetry 2012;151:379-85.
10. Van Engen RE, Young KC, Bosmans H, Thijssen M. European protocol for the quality control of the physical and technical aspects of mammography screening 2b digital mammography. In: European Guidelines for Quality Assurance in Breast Cancer Screening and Diagnosis (Perry N, Broeders M, de Wolf C, Tornberg S, Holland R, von Karsa L. Eds.) 4th ed. European Commission, Office for Official Publications of the European Communities, Luxembourg; 2006. p.11.
11. Thomas JA, Chakrabarti K, Kaczmarek R, Romanyukha A. Contrast-detail phantom scoring methodology. Med Phys 2005;32:807-14.
12. van derBurght R, Thijssen M, Bijkerk R. Manual Contrast-Detail Phantom CDMAM 3.4 & CDMAM Analyzer Software V 1.2 By, Version 7, Artinis Medical Systems BV. The Netherlands; 2010.
13. Young KC, Alsager A, Oduko JM. Evaluation of software for reading images of the CDMAM test objects to assess digital mammography systems. Proc SPIE 2008;6913:69131C.
14. E-Cabrera J, Brandan ME. Performance evaluation of a digital mammography unit using a contrast-detail phantom. J Phys Conf Ser 2015;582:012036.
15. Figl M, Semturs F, Kaar M, Hoffmann R, Floor-Westerdijk M, van der Burght R, *et al.* On the dose sensitivity of a new CDMAM phantom. Phys Med Biol 2015;60:N177-85.
16. Rivetti S, Lanconelli N, Campanini R, Bertolini M, Borasi G, Nitrosi A, *et al.* Comparison of different commercial FFDM units by means of physical characterization and contrast-detail analysis. Med Phys 2006;33:4198-209.
17. Konstantinidis AC. Cdmam_Fit_3: A graphical user interface for mammographic contrast – Detail analysis. E J Sci Technol e- Journal of Science & Technology 2014;9:20-7. Available from: http://www.e-jst.teiath.gr. [Last accessed on 2017 Oct 24].
18. Rojas LJ, Fausto AM, Mol AW, Velasco FG, Abreu PO, Henriques G, *et al.* Optimization of the exposure parameters in digital mammography using contrast-detail metrics. Phys Med 2017;42:13-8.
19. Fausto AM, Lopes MC, de Sousa MC, Furquim TA, Mol AW, Velasco FG, *et al.* Optimization of image quality and dose in digital mammography. J Digit Imaging 2017;30:185-96.
20. Samei E, Flynn MJ. An experimental comparison of detector performance for computed radiography systems. Med Phys 2002;29:447-59.
21. Samei E, Flynn MJ. An experimental comparison of detector performance for direct and indirect digital radiography systems. Med Phys 2003;30:608-22.
22. Samei E, Dobbins JT 3rd, Lo JY, Tornai MP. A framework for optimising the radiographic technique in digital X-ray imaging. Radiat Prot Dosimetry 2005;114:220-9.
23. Perry N, Broeders M, de Wolf C, Tornberg S, Holland R, von Karsa L. Executive summary. In: Perry N, Broeders M, de Wolf C, Tornberg S, Holland R, von Karsa L, editors. European Guidelines for Quality Assurance in Breast Cancer Screening and Diagnosis Supplements. 4th ed. Luxembourg: European Commission, Office for Official Publications of the European Union; 2013. p. 14-20.
24. Williams MB, Mangiafico PA, Simoni PU. Noise power spectra of images from digital mammography detectors. Med Phys 1999;26:1279-93.
25. Borasi G, Nitrosi A, Ferrari P, Tassoni D. On site evaluation of three flat panel detectors for digital radiography. Med Phys 2003;30:1719-31.
26. Salvagnini E, Bosmans H, Struelens L, Marshall NW. Effective detective quantum efficiency for two mammography systems: Measurement and comparison against established metrics. Med Phys 2013;40:101916.
27. Padgett R, Kotre CJ. Development and application of programs to measure modulation transfer function, noise power spectrum and detective quantum efficiency. Radiat Prot Dosimetry 2005;117:283-7.
28. Siewerdsen JH, Cunningham IA, Jaffray DA. A framework for noise-power spectrum analysis of multidimensional images. Med Phys 2002;29:2655-71.
29. Marshall NW. Early experience in the use of quantitative image quality measurements for the quality assurance of full field digital mammography x-ray systems. Phys Med Biol 2007;52:5545-68.
30. Ranger NT, Samei E, Dobbins JT 3rd, Ravin CE. Measurement of the detective quantum efficiency in digital detectors consistent with the IEC 62220-1 standard: Practical considerations regarding the choice of filter material. Med Phys 2005;32:2305-11.
31. Dance DR, Skinner CL, Young KC, Beckett JR, Kotre CJ. Additional factors for the estimation of mean glandular breast dose using the UK mammography dosimetry protocol. Phys Med Biol 2000;45:3225-40.
32. Bick U, Diekmann F. Digital Mammography. Springer, Berlin; 2010.
33. CIRS Tissue Simulation & Phantom Technology, The CIRS Model 011A Breast Phantom. Available from: http://www.cirsinc.com/011a_mammo.html/. [Last accessed on 2015 May 16].
34. Dance DR. Monte Carlo calculation of conversion factors for the estimation of mean glandular breast dose. Phys Med Biol 1990;35:1211-9.
35. Ferreira T, Rasband WS. 2010-2012. Image J User Guide-IJ 1.46. Available from: http://www.imagej.nih.gov/ij/docs/guide/. [Last accessed on 22015 Feb 02].